Global Elastic Response Simulation

Project Representative
Seiji Tsuboi Data Research Center for Marine-Earth Sciences, Japan Agency for Marine-Earth Science and Technology

Authors
Satoru Tanaka Institute for Research on Earth Evolution, Japan Agency for Marine-Earth Science and Technology
Seiji Tsuboi Data Research Center for Marine-Earth Sciences, Japan Agency for Marine-Earth Science and Technology

We compute theoretical seismic waves for realistic three dimensional (3-D) Earth models and recent large earthquake using Spectral-Element Method (SEM) and compare them with the observed seismic waves. We calculate synthetic seismic waveform for 2013 Sea of Okhotsk deep earthquake (Mw8.3) using fully 3-D Earth model. Our results indicate that the earthquake source mechanism of this event can be modeled by a rupture along low-dip fault. We also have calculated synthetic seismograms for Fiji deep earthquake and compared with the observed seismograms recorded in Europe. The results demonstrate that current performance of SEM is insufficient for the outermost core study using velocity seismograms and higher frequency contents up to at least 0.5 Hz are required, which we hope to be realized with the next generation Earth Simulator.

Keywords: Synthetic seismograms, 3-D velocity structure of the Earth, Spectral Element Method, Core-mantle structure

1. May 24, 2013 Sea of Okhotsk deep earthquake (Mw8.3)

May 24, 2013 Sea of Okhotsk earthquake (Mw 8.3, depth 640km NEIC) was not only one of the largest events in this general region but one of the largest deep earthquakes ever recorded (Fig. 1). We apply the waveform inversion technique to obtain slip distribution in the source fault of this earthquake in the same manner as our previous work (Nakamura et al., 2010 [1]). We use 57 broadband seismograms of IRIS GSN seismic stations with epicentral distance between 30 and 100 degrees. The broadband original data are integrated into ground displacement and band-pass filtered in the frequency band 0.002-1 Hz. We use the velocity structure model IASP91 to calculate the wavefield near source and stations. We assume that the fault is squared with the length 135 km. We obtain source rupture model for both nodal planes with high dip angle (81 degree) and low dip angle (10 degree) and compare the synthetic seismograms with the observations to determine which source rupture model would explain the observations better. We calculate broadband synthetic seismograms with this source propagation model for a realistic 3D Earth model using the spectral-element method (SEM) (Komatitsch and Tromp, 2002 [2]). The simulations are performed using 1014 processors, which require 127 nodes of the Earth Simulator 2. We use a mesh with 200 million spectral-elements, for a total of 13 billion global integration grid points. This translates into an approximate grid spacing of 2.0 km along the Earth's surface. On this number of nodes, a simulation of 30 minutes of wave propagation accurate at periods of 3.5 seconds and longer requires about 7 hours of CPU time. Comparison of the synthetic waveforms with the observation shows that source rupture model with the low dip angle fault plane explains the observation better specifically at stations, which locate south of the epicenter. These results demonstrate that the source rupture

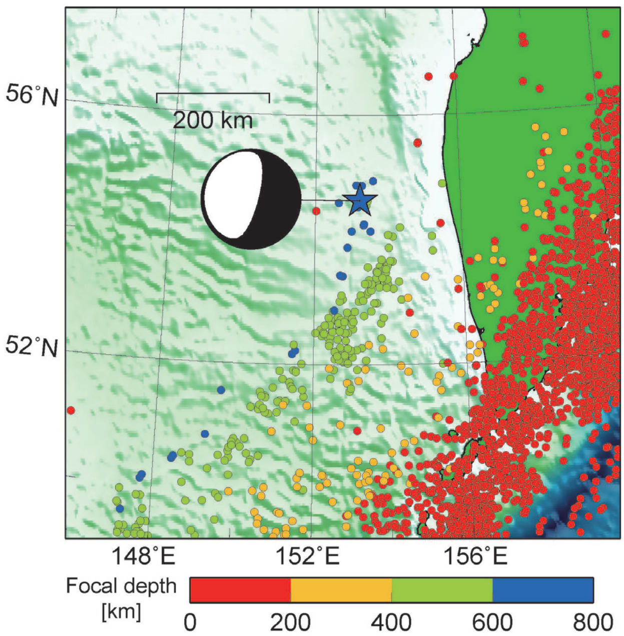

Fig. 1 Global CMT solution of 2013 Okhotsk deep earthquake and seismic activity of surrounding region. Epicenters are the earthquakes,which occurred during 1973 and September 2013 (Tsuboi et al., 2013 [3]).

of this deep earthquake occurred along the horizontal fault plane inside the subducting pacific plate.

We also have computed broadband synthetic seismograms using point source Global CMT solution and compared with the observation. Figures 2 show comparison of the synthetics with the observation for low-pass filtered traces and band-pass filtered traces. Synthetics for GCMT solution match the observation well in low frequencies but do not match well in

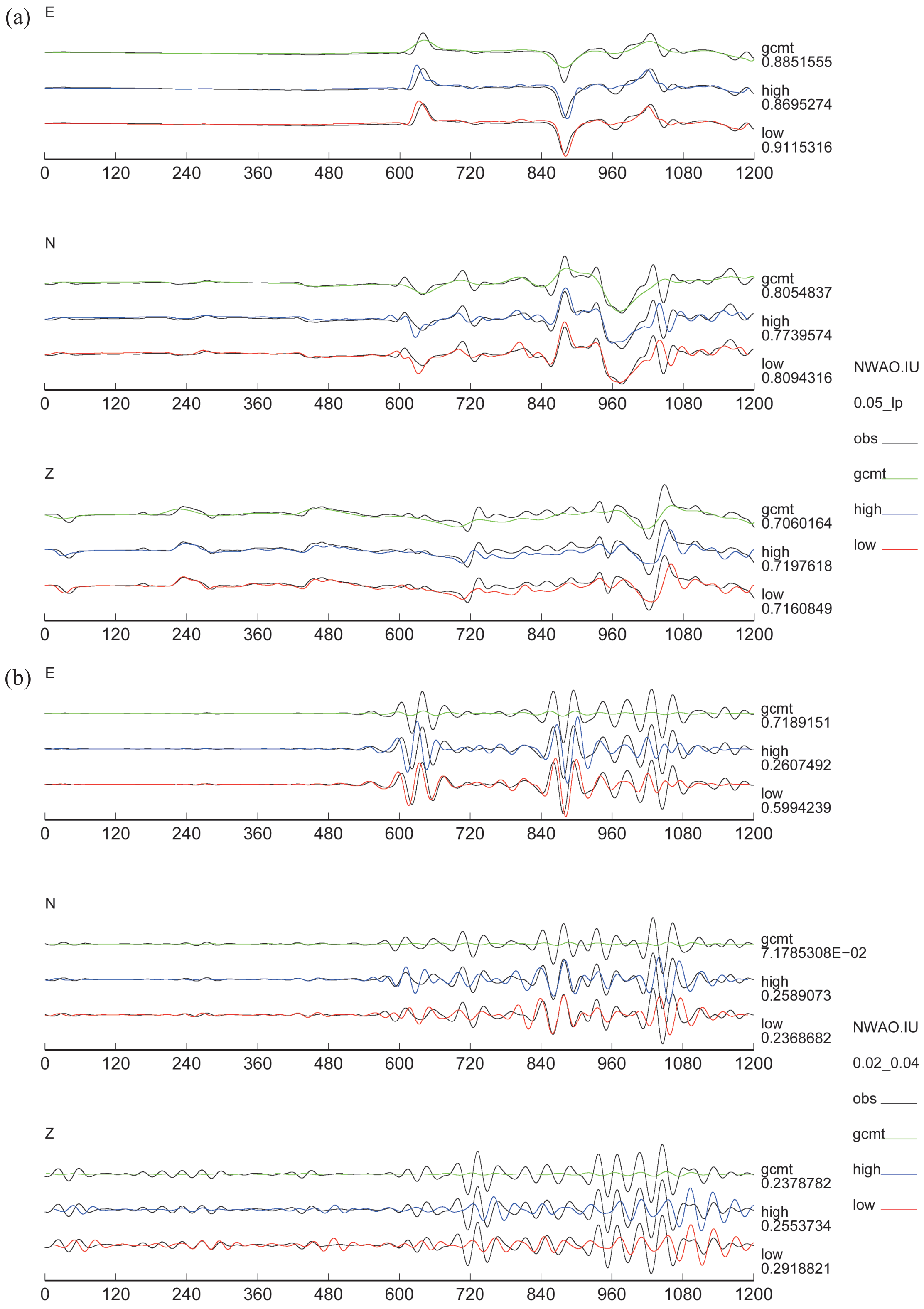

Fig. 2. (a) Comparison of synthetic seismograms for global CMT solution and finite fault model with observed seismograms. These traces are lowpass filtered at 20 second. Comparisons are displayed for EW components, NS components and vertical components from top to bottom. For each component, black traces are observed seismograms. Green traces are for global CMT solution, blue traces are for high-dip angle fault model and red traces are for low-dip angle fault model (Tsuboi et al., 2013) [3]). (b) Same as (a) but traces are bandpass filtered between 25 second and 50 second (Tsuboi et al., 2013 [3]).

high frequencies, which implies that this source mechanism contain much high frequency components. This may be consistent to the limited rupture area and large rupture velocity due to high rigidity (Tsuboi et al., 2013 [3]).

2. Seismological structure at the top of the Earth's outer core

Seismic structure at the top of the Earth's core is quite important to elucidate a stable stratification in the outermost part of the Earth's core. SmKS waves are most suitable for the observational constraints (Tanaka, 2007 [4]; Alexandrakis and Eaton, 2010 [5]; Helffrich and Kaneshima, 2010 [6]; Kaneshima and Helffrich, 2013 [7]; Fig. 3). Although the differential travel times between SmKS waves are analyzed to reduce the structural effect at the base of the mantle, it has been thought that the strong and unknown structure in the D" region certainly gives a bias in the estimation of the outer core structure (Garnero and Helmberger, 1995 [8]). For further studies, a relevant waveform modeling is required to find how to distinguish the structures above and below the core-mantle boundary.

To date, reflectivity method (RM) has been frequently used, which can easily synthesizes SmKS waves down to the period of 2 s at distances from 150-160° with 1-D structure, and can reproduce S5KS on velocity seismograms as previously noted by Helffrich and Kaneshima (2010) [6]. To fully incorporate 3D mantle heterogeneity, the spectral element method (SEM) can be used on Earth Simulator 2, which enables us to achieve the shortest period of about 3.5 s with 127 nodes (1014 CPUs). We adopt these setting and conduct the waveform modeling for PREM incorporating ETOPO5 and CRUST2.0 to simulate seismograms from a South Fiji earthquake observed by European seismic networks as a single large array (Fig. 4; Tanaka (2013) [9]). The phase-weighted stack is applied and the differential travel times are picked. Comparing between displacement seismograms from RM (only PREM is used) and SEM, differential travel times of S4KS–S3KS and S3KS–S2KS are coincides within 0.1 s that is two sampling intervals (Figs. 5 and 6; Tanaka (2014) [9]). However, the differential travel time of S4KS–S3KS on velocity seismogram with SEM was 0.5 s larger than that with RM. Furthermore, S5KS phase is not identified on velocity seismogram with SEM (Figs. 7 and 8; Tanaka (2013) [9]). These suggest that the current setting of SEM is insufficient for the outermost core study using velocity seismograms and higher frequency contents up to at least 0.5 Hz are required, which we hope to be realized with the next generation Earth Simulator.

Additionally we have conducted another runs incorporating the 3D mantle models of S20RTS with the spherical harmonics coefficients at the base of the mantle modified to be 3 times and an approximated SB4L18. These results clearly show that there are strong effects of heterogeneity in the lowermost mantle on the differential travel times of S4KS–S3KS and S3KS–S2KS (Figs 7, 8, and 9; Tanaka (2014) [9])

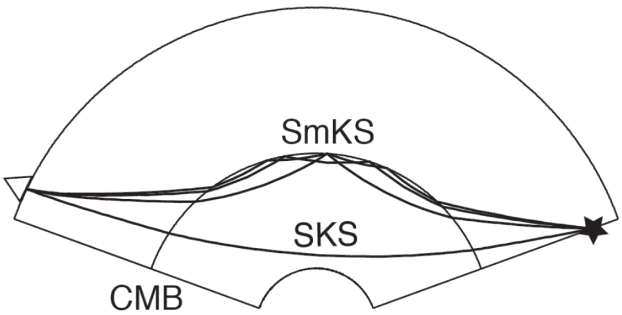

Fig. 3 Seismic ray paths of SKS, SmKS waves.

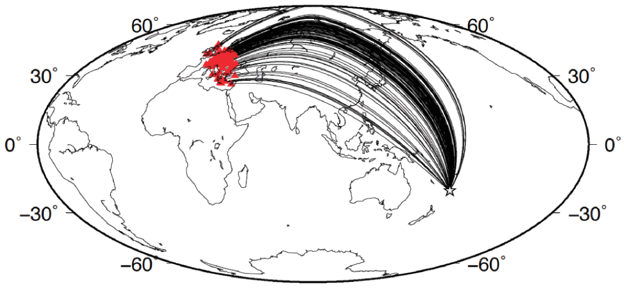

Fig. 4 Geographical distribution of epicenter and stations used for the calculation of synthetic waveforms.

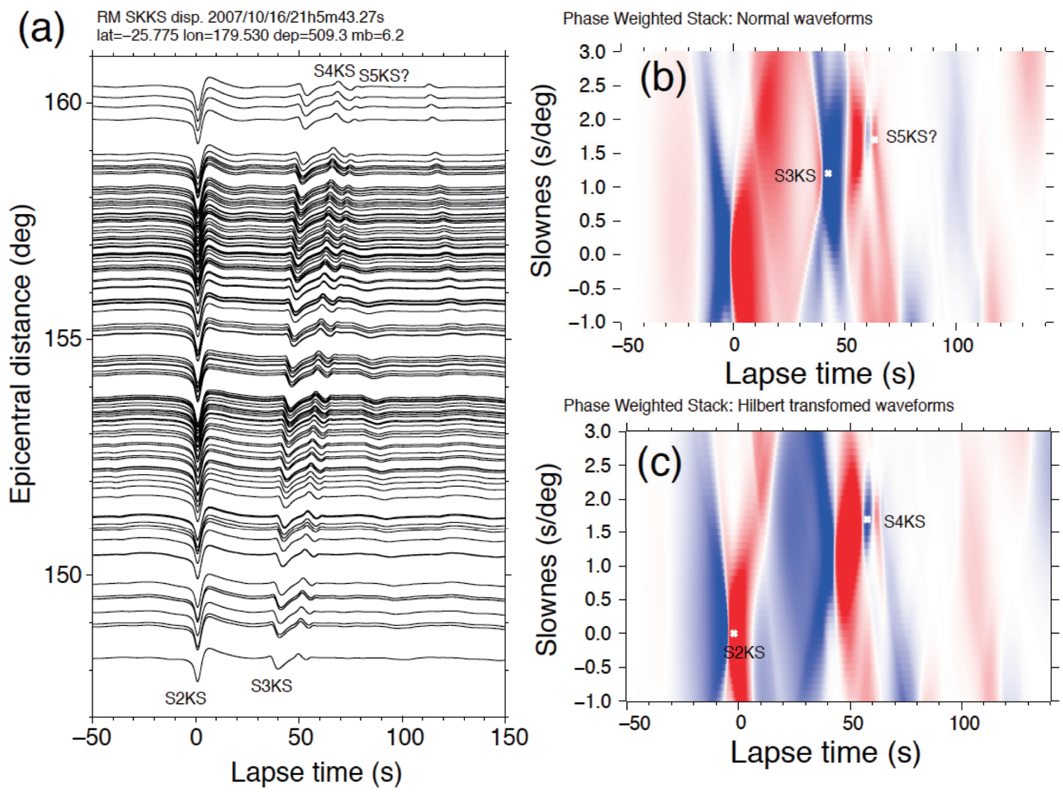

Fig. 5 (a) Displacement waveforms of S2KS and later phases synthesized by reflectivity method. PREM is used. (b) Vespagram by phase weighted stack with power index of 2 using original waveforms, in which the peak of S3KS is marked by a white cross. (c) Vespagram by phase weighted stack using Hilbert transformed waveforms, in which the peaks of S2KS and S4KS are marked by white crosses.

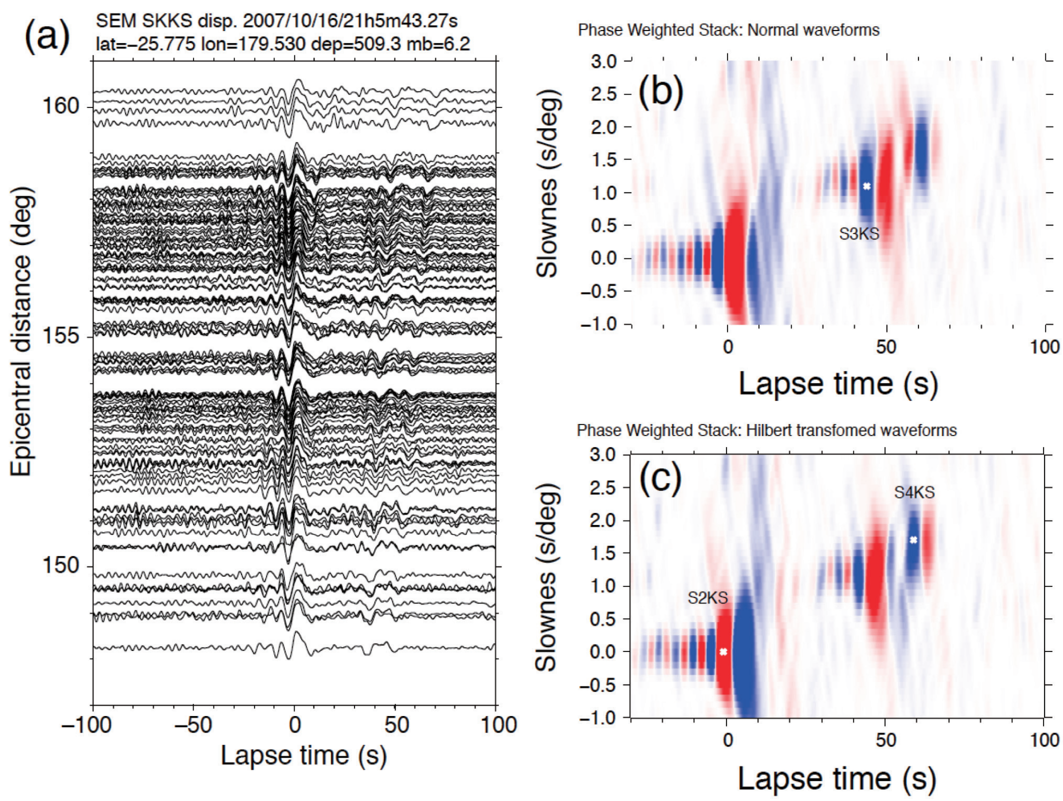

Fig. 6 Same as Fig. 5 except that spectral element method is used for the waveform calculation.

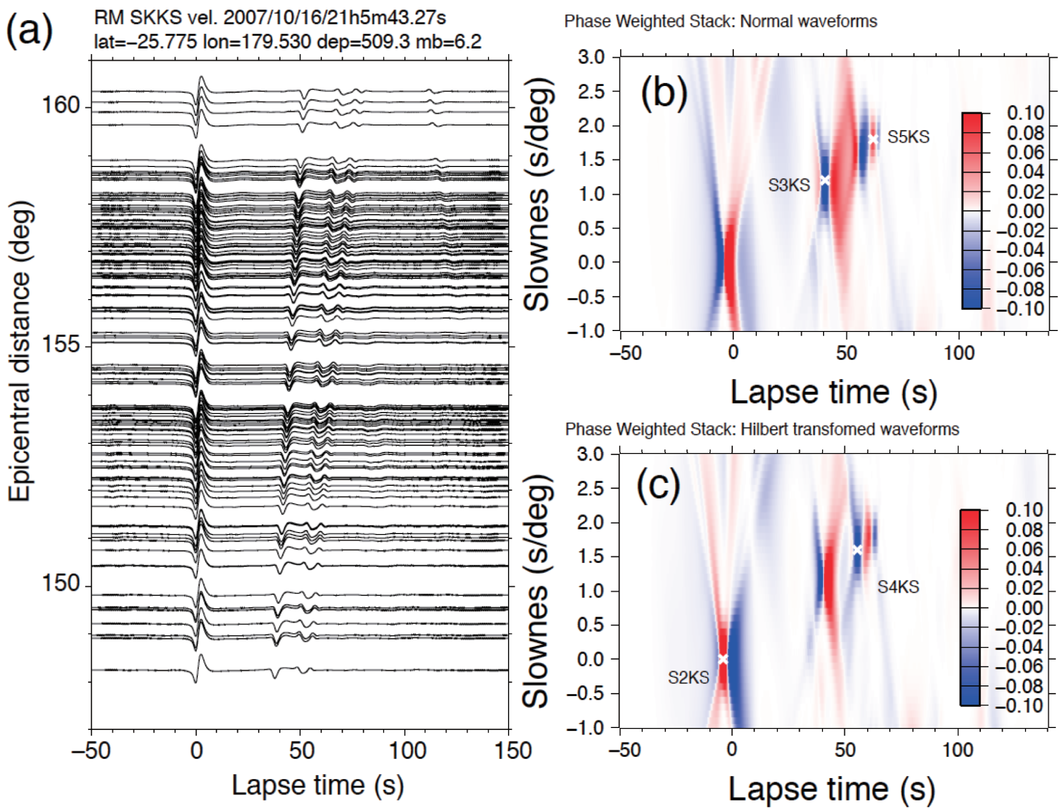

Fig. 7 Same as Fig. 5 except for velocity waveform.

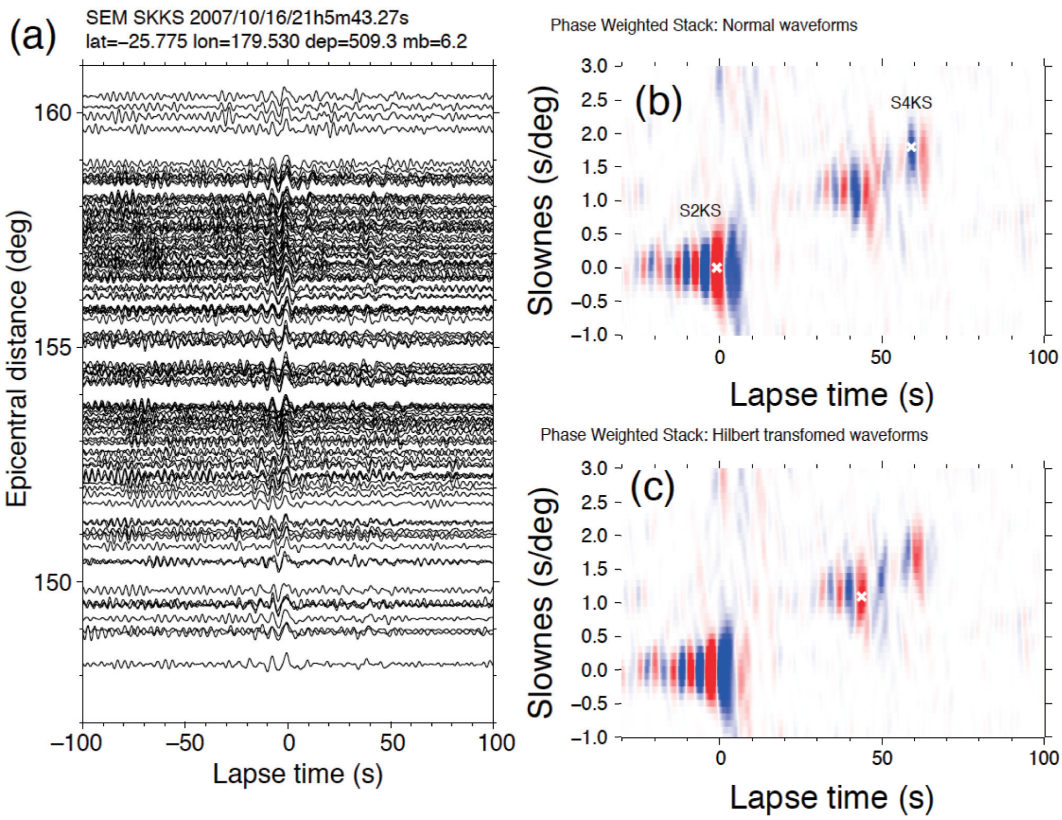

Fig. 8 Same as Fig. 6 except for velocity waveform.

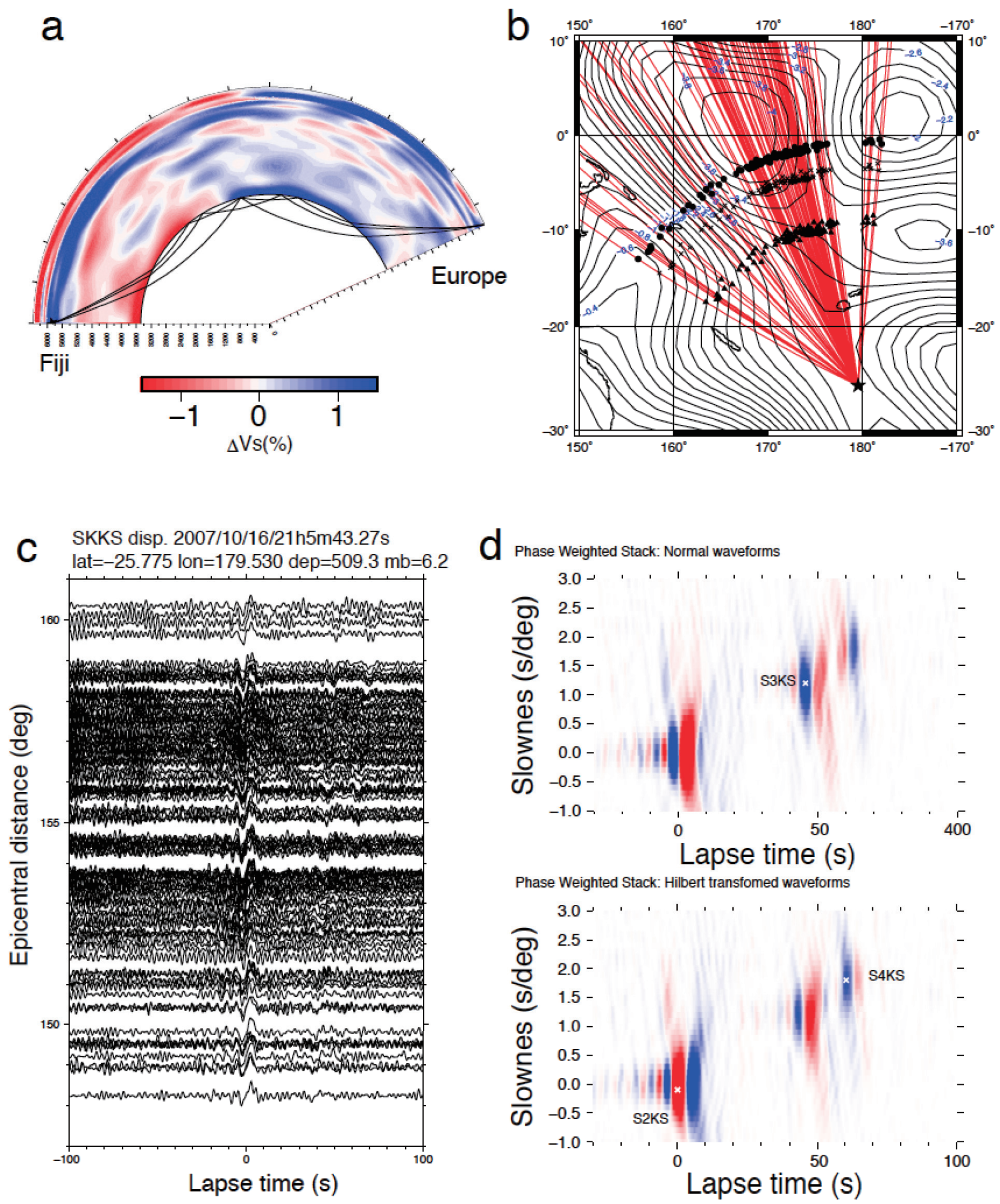

Fig. 9 (a) Vertical cross-section from the hypocenter to a station with seismic ray paths of SmKS. The background color indicates the heterogeneity in the mantle that is calculated with S20RTS but the coefficients at the base of the mantle are multiplied by factor 3. (b) Geographical distribution of SmKS piercing points at the core-mantle boundary beneath the hypocentral area. Triangles, crosses, and circles represent the points of S2KS, S3KS, and S4KS, respectively. (c) Displacement waveforms SmKS synthesiezed by spectral element method with S20RTS but the coefficients at the base of the mantle are multiplied by factor 3. (d) Vespagrams of S2KS and later phases.

References

[1] Nakamura, T., Tsuboi, S., Kaneda, Y., and Yamanaka, Y., 2010. Rupture process of the 2008 Wenchuan, China earthquake inferred from teleseismic waveform inversion and forward modeling of broadband seismic waves, Tectonophysics, 491, 72-84.

[2] Komatitsch, D. and Tromp, J., 2002. Spectral-element simulations of global seismic wave propagation-I. Validation. Geophys. J. Int. 149, 390-412.

[3] Tsuboi, S., Miyoshi, T., Nakamura, T., Obayashi, M., and Tono, Y., 2013. Source mechanism of May 24, 2013 Sea of Okhotsk deep earthquake (Mw8.3) estimated by broadband waveform modeling, AGU Fall meeting, S41-C07.

[4] Tanaka, S., 2007. Possibility of a low P-wave velocity layer in the outermost core from global SmKS waveforms, Earth Planet. Sci. Lett., 259, 486-499.

[5] Alexandrakis, C. and D. W. Eaton, 2010. Precise seismic-wave velocity atop Earth's core: No evidence for outer-core stratification, Phys Earth Planet In, 180(1-2), 59-65, doi:10.1016/j.pepi.2010.02.011.

[6] Helffrich, G. and S. Kaneshima, 2010. Outer-core compositional stratification from observed core wave speed profiles, Nature, 468(7325), 807-U896, doi:10.1038/nature09636.

[7] Kaneshima, S. and G. Helffrich, 2013. Vp structure of the outermost core derived from analysing large-scale array data of SmKS waves, Geophys J Int, 193(3), 1537-1555, doi:10.1093/gji/ggt042.

[8] Garnero, E. J. and D. V. Helmberger,1995. On seismic resolution of lateral heterogeneity in the Earth's outermost core, Phys. Earth Planet. Inter., 88(2), 117-130.

[9] Tanaka, S., 2014. Broadband waveform modeling with the spectral element method on Earth Simulator for the study of the structure at the top of the Earth's outer core, accepted, JAMSTEC-R.

全地球弾性応答シミュレーション

課題責任者
坪井　誠司　　海洋研究開発機構　地球情報研究センター
著者
田中　　聡　　海洋研究開発機構　地球内部ダイナミクス領域
坪井　誠司　　海洋研究開発機構　地球情報研究センター

スペクトル要素法により現実的な3次元地球モデルに対する理論地震波形記録を2013年千島沖地震（Mw8.3）に対して計算した。計算は地球シミュレータの127ノードを用いて、周期約5秒の精度で行った。理論地震波形は、低角逆断層と高角逆断層の震源過程モデルに対して計算し、それぞれを観測と比較した結果、低角逆断層の震源モデルが観測をより良く説明出来ることが分かった。また、点震源のGCMT解を用いた理論波形との比較では、短周期側で観測を説明出来ないことが分かったが、これは、この地震の震源過程が短周期成分を多く含んでいる可能性があることを示している。

フィジーで起きた深発地震により励起された地震波をヨーロッパ大陸に展開された地震網で観測した波形に対してスペクトル要素法による理論地震波形計算を行った。計算した理論地震波形の精度は核マントル境界の詳細な構造を推定するためには十分ではなく、少なくとも周期2秒の精度が必要であることが分かった。

キーワード: 理論地震波形記録, 3次元地球内部構造, スペクトル要素法, 核マントル境界